symmetry

IMPACT FACTOR 1.256

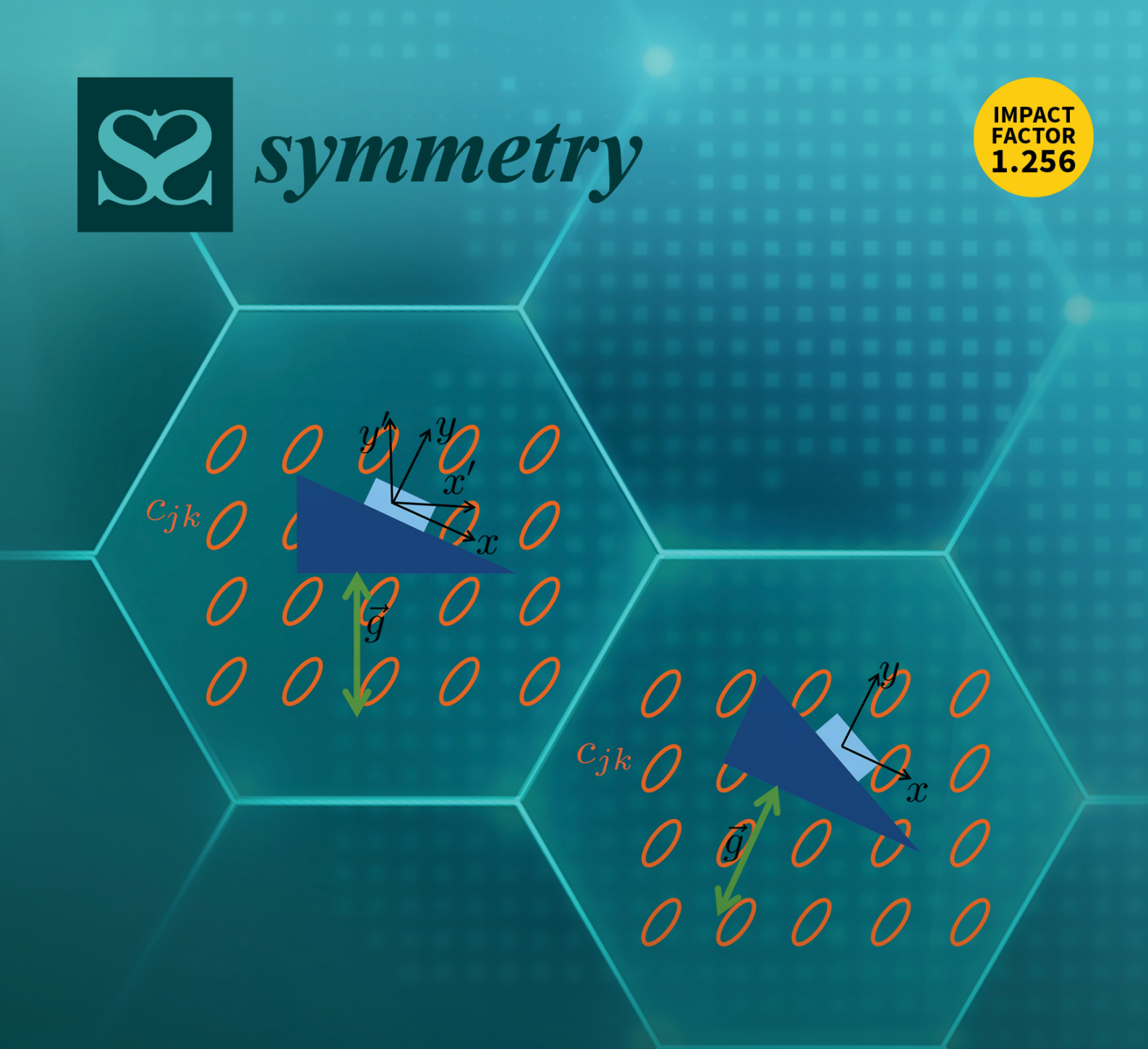

Spacetime Symmetries and Classical Mechanics

Volume 11 · Issue 1 | January 2019

MDPI

mdpi.com/journal/symmetry
ISSN 2073-8994

symmetry

MDPI

Article

Spacetime Symmetry and LemaîTre Class Dark Energy Models

Irina Dymnikova [1,2,*] and Anna Dobosz [2]

[1] A.F. Ioffe Physico-Technical Institute, Politekhnicheskaja 26, St. Petersburg 194021, Russia
[2] Department of Mathematics and Computer Science, University of Warmia and Mazury, Słoneczna 54, 10-710 Olsztyn, Poland; dobosz@uwm.edu.pl
* Correspondence: irina@uwm.edu.pl; Tel.: +48-601-362-059

Received: 14 December 2018; Accepted: 11 January 2019; Published: 15 January 2019

Abstract: We present the regular cosmological models of the Lemaître class with time-dependent and spatially inhomogeneous vacuum dark energy, which describe relaxation of the cosmological constant from its value powering inflation to the final non-zero value responsible for the present acceleration in the frame of one self-consistent theoretical scheme based on the algebraic classification of stress-energy tensors and spacetime symmetry directly related to their structure. Cosmological evolution starts with the nonsingular non-simultaneous de Sitter bang, followed by the Kasner-type anisotropic expansion, and goes towards the present de Sitter state. Spacetime symmetry provides a mechanism of reducing cosmological constant to a certain non-zero value involving the holographic principle which singles out the special class of the Lemaître dark energy models with the global structure of the de Sitter spacetime. For this class cosmological evolution is guided by quantum evaporation of the cosmological horizon whose dynamics entirely determines the final value of the cosmological constant. For the choice of the density profile modeling vacuum polarization in a spherical gravitational field and the GUT scale for the inflationary value of cosmological constant, its final value agrees with that given by observations. Anisotropy grows quickly at the postinflationary stage, then remains constant and decreases to $A < 10^{-6}$ when the vacuum density starts to dominate.

Keywords: dark energy; spacetime symmetry; de Sitter vacuum

1. Introduction

Observational data convincingly testify that our Universe is dominated at above 72% of its density by a dark energy with a negative pressure $p = w\rho$, $w < -1/3$ [1–4] (for a review [5]), with the best fit $w = -1$ corresponding to the cosmological constant λ associated with the vacuum density $\rho_{vac} = (8\pi G)^{-1}\lambda$ [6–11]. However, the Einstein cosmological term $\lambda g_{\mu\nu} = 8\pi G\rho_{vac}g_{\mu\nu}$ cannot be associated with the vacuum dark energy, for two reasons: (i) The quantum field theory estimates ρ_{vac} by $\rho_{Pl} = 5 \times 10^{93}$ g cm^{-3}. Confrontation of this estimate with the observational value $\rho_{obs} \simeq 1.4 \times 10^{-123}\rho_{Pl}$ produces the fine-tuning problem [12]. (ii) A large value $\Lambda = 8\pi G\rho_{vac}$ is needed for powering the inflationary stage of the Universe evolution, the observational data yield its much smaller today value, while the Einstein equations require $\rho_{vac} = const$.

The Planck density ρ_{Pl} provides a natural cutoff on zero-point quantum vacuum fluctuations in QFT which give rise to ρ_{vac} [12], as well as on applicability of classical General Relativity [13]. Proposals to solve the fine-tuning problem typically go beyond the classical General Relativity and involve both its quantization and modifications and extensions on the classical level.

As early as in 1978 Hawking supposed that quantum fluctuations in spacetime topology at small scales may provide a mechanism for vanishing a cosmological constant [14]. The point is that at the very short distances a spacetime itself undergoes uncertainties typical for quantum systems that implies impossibility to determine simultaneously a spacetime geometry and its changes. According

to Wheeler, spacetime beyond the Planck scale has foam-like structure and may involve substantial changes in geometry and topology [13] including, in particular, quantum wormholes [15,16].

On the other hand, the effective field theory still valid near the Planck energy scale, and the question why the observed cosmological constant is so small as compared with ρ_{Pl} is equivalent to the question why the universe is accelerating at present [17]. In default of a some fundamental symmetry which would reduce the value of λ to zero, most of proposals were focused on searching for physical mechanisms which could provide its small value today.

The Causal Entropic Principle, which requires disregarding the causally disconnected spacetime regions and maximizing the entropy produced within a causally connected region, has been applied for calculation the expected value for a present cosmological constant in [18] in the reasonable agreement with its observational value. Causality arguments were also used for analysis of relaxation of the cosmological constant to its present value in the context of the eternal inflation in the multiverse and a string landscape [19].

The non-singular model with the curvature square term, a cosmological term and a dilaton field ϕ has been proposed in [20]. In this model the effective potential for a dilaton field demonstrates the proper behavior to provide a successful inflationary stage with a graceful exit in the regime $\phi \to \infty$, and a small value of the vacuum density responsible for the late time acceleration in the regime $\phi \to -\infty$, that appears as the "threshold" for the universe creation [20].

A way to solution of the fine-tuning problem involving the Higgs boson as the most likely candidate for the inflaton field, has been proposed in [17] on the basis of an energy exchange between the inflaton field and a time-dependent Λ. Although the mass of the Higgs boson is much smaller than that needed for an inflaton, the hierarchy problem has been solved by introducing a coupling between $\Lambda(t)$ and the inflaton field, which even in the simplest form, $\mathcal{L}_{int} \sim \phi\Lambda$, can provide a solution of the fine-tuning problem [17].

In the framework of the QFT model with a scalar and a fermion field and a physical cutoff rendering the QFT finite it has been shown that the violation of the Lorentz invariance at the high momentum scale can be made consistent with a suppression of the violation of the Lorentz invariance at the low momenta. The fine tuning required to provide both the suppression and the existence of a light scalar particle in the spectrum has been determined at the one loop level [21].

In the paper [22] it was noted that the extreme smallness of the gravitational fine structure constant $\alpha_g = \sqrt{G\hbar\Lambda/c^3} = 1.91 \times 10^{-61}$ ($\rho_{vac}/\rho_{Pl} = (1/8\pi)\alpha_g$) may suggest an essentially different structure of a dark energy, which could not be entirely described by a cosmological constant.

The cosmological constant provides the empirically verified explanation for the present accelerated expansion. The ΛCDM model includes a cosmological constant, inflationary initial conditions, cold dark matter, standard radiation and neutrino content and $\Omega_{tot} = 1$, and demonstrates a good agreement with the current cosmological observations [23]. Extensions of the ΛCDM model, abbreviated as $I\Lambda CDM$, involve the vacuum energy interacting with the cold dark matter [24,25] (for a recent review [26]). However, theoretical difficulties including the fine-tuning problem [27,28] enforced looking for alternative models of a dark energy (for a review [29]).

Most of the alternative models introduce a dark energy of a non-vacuum origin which behaves like a cosmological constant when needed. Various models have been developed (for a review [30–33]) and checked out by the cosmography tests [34,35]. Among them phenomenological quintessence models with $-1 < w < -1/3$ [4] and quintom models with two dynamical scalar fields, a canonical field and a phantom field with $w < -1$ [36], supported by symmetry requirements [37], present the dynamically viable dark energy models (for a dynamical analysis of the quintom models [38]).

Modified gravity models (for a review [39]) involve screening mechanisms that are characterized by an effective value of the gravitational coupling G_N for the regions with the different gravitational potentials; the model predictions approach those typical for General Relativity in the regions of a strong gravitational field [29].

A general approach to the viable modified F(R) gravity describing the inflation and the current accelerated expansion has been developed in [40] including investigation of the exponential models of the modified gravity.

The holographic dark energy models [41,42] establish that the QFT ultraviolet cutoff produces the dark energy density $\rho_{DE} = 3C^2 M_{Pl}^2 L^{-2}$ [43], where C is a numerical constant and L indicates the infrared cutoff ([44] and references therein). The scale L^{-1} can be considered as the Hubble scale since the resulting density is comparable with the current dark energy density [45,46]. Another option for L is the particle and future horizons as the generalized holographic dark energy models for a specific $f(R)$ gravity model ([47] and references therein). In [48] a holographic dark energy model has been constructed for the apparent horizon in a curved universe. The holographic models for the particle and future horizons have been analyzed in [49] with the conclusion that the future horizon presents more similarities with the dark energy behavior.

Models with $-1 < w < -1/3$ have been thoroughly tested with using the WMAP (Wilkinson Microwave Anisotropy Probe) - CMB (Cosmic Microwave Background) data, which gave the constraint $w_Q \leq -0.7$ and the best fit $w_Q = -1$ [6–8,11]. CMB measurements [50] together with the BAO (Baryon Acoustic Oscillations) data [51] and SNe (SuperNovae) Ia data [52] confirmed this result giving $w = -1.06 \pm 0.06$ at 68% CL [51].

Model-independent evidence for the character of the dark energy evolution obtained from the BAO data distinguish theories with relaxation of Λ from a large initial value [53].

Relaxation of Λ has been considered in [54] on the basis of the adjustment mechanism proposed in [55] in the model extending General Relativity by adding a class of the invariant terms that reduce an arbitrary initial value of the cosmological constant to a needed value.

A unified description of the dark energy driving both the inflationary stage and the current accelerated expansion is presented in [56] on the basis of a quadratic model of gravity which includes an exponential F(R) gravity contribution with the high-curvature corrections coming from the higher-derivative quantum gravity beyond the one-loop approximation.

Let us note that although the cosmological constant provides the convincing explanation for the observed accelerated expansion, a clear justification of its small value does not exist until now [49].

In this paper we outline our approach to relaxation of a cosmological constant in the frame of the model-independent self-consistent theoretical scheme which makes cosmological constant intrinsically variable. A vacuum dark energy is introduced in general setting suggested by the algebraic classification of stress-energy tensors and directly related to spacetime symmetry that provides a mechanism of reducing a cosmological constant to a certain non-zero value involving the holographic principle which singles out the special class of the Lemaître cosmological models with the global structure of the de Sitter spacetime.

The quantum field theory in a curved spacetime does not contain a unique specification for the vacuum state of a system, and the symmetry of the vacuum expectation value of a stress-energy tensor does not always coincide with the symmetry of the background spacetime ([57] and references therein, for a detailed discussion [58]). What is more important, QFT does not contain an appropriate symmetry to zero out the cosmological vacuum density or to reduce it to a non-zero value.

The key point is that a relevant symmetry does exist in General Relativity as a spacetime symmetry, directly related to the algebraic structure of stress-energy tensors which determine the spacetime geometry as source terms in the Einstein equations. Algebraic classification of stress-energy tensors [59,60] suggests a model-independent definition of a vacuum as a medium by the algebraic structure of its stress-energy tensor and admits the existence of vacua whose symmetry is reduced as compared with the maximally symmetric de Sitter vacuum associated with the Einstein cosmological term $T_k^i = \rho_{vac}\delta_k^i$ ($p = -\rho_{vac}$; $\rho_{vac} = \text{const}$ by $T_{k;i}^i = 0$) and responsible for the de Sitter geometry which ensures accelerated expansion, isotropy and homogeneity independently of specific properties of the particular models for ρ_{vac} [61,62]. To make Λ variable it is enough to reduce symmetry of $T_k^i = \rho_{vac}\delta_k^i$ while keeping its vacuum identity ($p_k = -\rho$ for one of two spatial directions) [63,64]. The cosmological

constant Λ becomes a time component Λ^t_t of a variable cosmological term $\Lambda^i_k = 8\pi G T^i_k$ [65], which allows a vacuum energy density to be intrinsically dynamical, i.e., time-evolving and spatially inhomogeneous (by virtue of $\Lambda^i_{k;i} = 0$).

A stress-energy tensor T^i_k with a reduced symmetry represents an intrinsically anisotropic vacuum dark fluid which can be evolving and clustering, and provides the unified description of dark energy and dark matter based on the spacetime symmetry [64,66] (for a review [67]). The relevant spherical solutions to the Einstein equations are specified by $T^t_t = T^r_r$ $(p_r = -\rho)$ and belong to the Kerr-Schild class. Regular spherical solutions satisfying the weak energy condition, which implies non-negativity of density as measured by an observer on a time-like curve, have obligatory de Sitter centers, $T^i_k = (8\pi G)^{-1}\Lambda\delta^i_k$. They describe regular cosmological models with time-evolving and spatially inhomogeneous vacuum dark energy, and compact vacuum objects generically related to a dark energy via their de Sitter vacuum interiors: regular black holes, their remnants and self-gravitating vacuum solitons, which can be responsible for observational effects typically related to a dark matter [64,68].

This implies a natural phenomenological inclination with the ΛCDM model: Primordial black hole remnants are considered as (cold) dark matter candidates for more than three decades [69,70]. The problem with singular black holes concerns the existence of the viable products of their evaporation ([71] and references therein). Quantum evaporation of the regular black holes (RBH) involves a 2-nd order phase transition followed by quantum cooling and resulting in thermodynamically stable remnants ([72] and references therein; for a review [73]). Primordial RBH remnants and self-gravitating vacuum solitons appear at the phase transitions in the early universe where they can capture available de Sitter vacuum in their interiors and form graviatoms binding electrically charged particles [74]. Their observational signatures as heavy dark matter candidates generically related to a vacuum dark energy include the electromagnetic radiation whose frequency depends on the scale of the interior de Sitter vacuum, within the range $\sim 10^{11}$ GeV available for observations [68,74]. In graviatoms with the GUT scale interiors, where the baryon and lepton numbers are not conserved, the remnant components of graviatoms can induce the proton decay, which could in principle serve as their additional observational signature in heavy dark matter searches at the IceCUBE experiment [68].

Regular cosmological models with the vacuum dark energy belong to the Lemaître class of cosmological models and are able to describe evolution between different states dominated by the de Sitter vacuum [58]. There exists infinitely many distributions of matter which satisfy $R_{ik} = \Lambda g_{ik}$ and hence model the cosmological constant [75], but in all cases it is ultimately de Sitter vacuum drives the accelerated expansion due to the basic properties of the de Sitter geometry, independently on an underlying particular model for Λ. In a similar way a dynamical vacuum dark energy associated with a variable cosmological term, generates geometries whose basic properties involve in the natural way restoration of the spacetime symmetry asymptotically or/and at certain stages of the universe evolution. Such geometries describe the relaxation of the cosmological constant by the Lemaître class anisotropic cosmological models, which reduce to the isotropic FLRW models at the stages with the spacetime symmetry restored to the de Sitter group. This makes it possible to describe on the common ground the currently observed accelerated expansion and the inflationary stages predicted by the standard model and related to the phase transitions in the universe evolution [76]. Such a model involving the GUT and QCD vacuum scales has been presented in [58] on the basis of the phenomenological density profile with the typical behavior for a cosmological scenario with an inflationary stage followed by decay of the vacuum energy described by the exponential function. The model parameters characterizing the decay rate are uniquely fixed by the requirements of the causality and analyticity. Other model parameters are fixed by the values ρ_{GUT}, ρ_{QCD}, the currently observed density ρ_λ and $\Omega = 1$. The only remaining free parameter, the e-folding number for the first inflation, was estimated by the observational constraints on the CMB anisotropy. It was shown that the Lemaître class cosmological model with the vacuum dark fluid can describe the universe evolution in the frame of one theoretical scheme which fairly well conforms to the basic observational features [58].

The spacetime symmetry provides a mechanism of reducing the cosmological constant to a certain non-zero value. The holographic principle distinguishes the special class of the Lemaître dark energy models, for which the cosmological evolution is guided by the quantum evaporation of the cosmological horizon whose dynamics entirely determines the final value of the cosmological constant.

Here we present the basic features of the Lemaître class dark energy models and outline in some detail the special class of models singled out by the holographic principle. Section 2 presents the spherically symmetric vacuum dark fluid and the generic properties of the spacetime generated by the vacuum dark energy. Section 3 presents the basic equations and the generic properties of the Lemaître class cosmological models with the vacuum dark energy, and the special class of the Lemaître models favored by the holographic principle, including the detailed behavior of the anisotropy parameter in the course of the universe evolution. Section 4 contains summary and discussion.

2. Algebraic Structure of Tress-Energy Tensors for Vacuum Dark Energy and Spacetime Symmetry

Stress-energy tensors of the spherically symmetric vacuum dark fluid have the algebraic structure defined by [63]

$$T_t^t = T_r^r \ \ (p_r = -\rho); \ \ T_\theta^\theta = T_\phi^\phi. \tag{1}$$

The equation of state, following from the conservation equation $T^k_{i;k} = 0$, reads [63,77] $p_r = -\rho$; $p_\perp = -\rho - \frac{r}{2}\rho'$, where $\rho(r) = T_t^t$ is the energy density, $p_r(r) = -T_r^r$ is the radial pressure, and $p_\perp(r) = -T_\theta^\theta = -T_\phi^\phi$ is the transversal pressure for the anisotropic vacuum dark fluid [64]. The stress-energy tensors specified by (1) generate, as the source terms in the Einstein equations, the globally regular spacetimes with the de Sitter centre (replacing the Schwarzschild singularity) provided that the weak energy condition (WEC) is satisfied [78,79]. The spacetime symmetry breaks from the de Sitter group in the origin [78].

The early proposals of replacing a singularity with the de Sitter core were based on the hypotheses of a self-regulation of the geometry by the vacuum polarization effects [77], of the existence of the limiting curvature [80], and of the symmetry restoration at the GUT scale in the course of the gravitational collapse [63,81]. Later a loop quantum gravity and the noncommutative geometry provided arguments in favor of a de Sitter interior in place of a singularity [82–87].

A metric generated by a source term specified by (1) belongs to the Kerr-Schild class [88]

$$ds^2 = g(r)dt^2 - \frac{dr^2}{g(r)} - r^2 d\Omega^2. \tag{2}$$

For the regular spherical solutions with the de Sitter centre WEC leads to monotonical decreasing of the density profile $\rho(r)$ [78]. In the case of two vacuum scales we can thus separate in T_t^t the background vacuum density $\rho_\lambda = (8\pi G)^{-1}\lambda$, introducing $T_t^t(r) = \rho(r) + \rho_\lambda$, where $\rho(r)$ is a dynamical density decreasing from the value at the center $\rho_\Lambda = (8\pi G)^{-1}\Lambda$ to zero at infinity; T_t^t evolves from $(8\pi G)^{-1}(\Lambda + \lambda)$ to $(8\pi G)^{-1}\lambda$ and provides the intrinsic relaxation of a cosmological constant. The metric function [89]

$$g(r) = 1 - \frac{2G\mathcal{M}(r)}{r} - \frac{\lambda r^2}{3}; \quad \mathcal{M}(r) = 4\pi \int_0^r \rho(x)x^2 dx \tag{3}$$

is asymptotically de Sitter with λ as $r \to \infty$ and with $(\Lambda + \lambda)$ as $r \to 0$.

Geometry has three basic length scales: $r_g = 2GM$ ($M = 4\pi \int_0^\infty \rho r^2 dr$); $r_\Lambda = \sqrt{3/\Lambda}$; $r_\lambda = \sqrt{3/\lambda}$, and an additional length scale $r_* = (r_\Lambda^2 r_g)^{1/3}$ characteristic for the geometry with the de Sitter interior. The relation of r_λ to r_Λ represents the characteristic parameter relating two vacuum scales $q = r_\lambda / r_\Lambda = \sqrt{\Lambda/\lambda} = \sqrt{\rho_\Lambda/\rho_\lambda}$.

Let us note that the characteristic scale $r_* = (r_\Lambda^2 r_g)^{1/3}$, introduced first in [77] as related to a self-regulation of the geometry, appears explicitly in the simple semiclassical model of the vacuum

polarization in the spherical gravitational field based on the fact that all fields are involved in a collapse, therefore all of them contribute to the stress-energy tensor and hence to geometry [63,78,90]. The scale r_* defines the zero gravity surface at which the strong energy condition is violated [63,90]. In thermodynamics of regular black holes this scale determines evolution during evaporation [72]. In the Nonlinear Electrodynamics coupled to Gravity the existence of zero gravity surface inside a regular compact object allows to present a certain explanation of the appearance of the minimal length scale in the electromagnetic reaction of the electron-positron annihilation [91].

In the Schwarzschild-de Sitter spacetime the similar scale with the background λ appears in the minimum of the metric function $g(r)$ (with $\mathcal{M}(r) = M = const$) for the Kottler-Trefftz geometry [92], and defines the boundary beyond which there are no bound orbits for test particles [93,94]. This scale plays the fundamental role in the non-linear theories of massive gravity. The original model by Fierz and Pauli described a massive spin-2 particle in the Minkovski space involving five degrees of freedom but was incompatible with the Solar System tests. Nonlinear extensions of this theory, proposed first by Vainshtein [95] include the mechanism of hiding some degrees of freedom and restoring General Relativity below a certain scale r_v called the Vainshtein radius which marks the transition to the regions where the extra degrees of freedom become essential at the large distances ([96,97] and references therein). In the cosmological context the Vainshtein scale r_v involves the background λ and plays the role of the astrophysical scale set by the cosmological constant λ as it was shown in [98] where the general conditions were derived applicable for any theory of massive gravity and responsible for the coincidence of r_v with the relevant scale for the Schwarzshild-de Sitter spacetime obtained in the GR frame with the dynamical metric involving all degrees of freedom. In the context of black hole thermodynamics the basic conditions for an observer in massive gravity [99] provide agreement of the obtained there results with those obtained in GR.

In the considered context of regular spacetimes with the vacuum dark energy the number of the vacuum scales determines the maximal number of the horizons. In accordance with the Einstein equations, the pressure $p_\perp$ is related with the metric function $g(r)$ as

$$8\pi G p_\perp = \frac{g''}{2} + \frac{g'}{r}. \tag{4}$$

It follows that an extremum of $g(r)$ in the region where $p_\perp > 0$, is a minimum. The transversal pressure $p_\perp$ becomes negative in the vicinity of the de Sitter center with the characteristic scale r_Λ and in the asymptotically de Sitter region of large r with the scale r_λ. Then there exists only one region where $p_\perp > 0$. Since $g(r)$ has different signs at $r \to 0$ and $r \to \infty$, the single minimum of $g(r)$ implies the existence of at most 3 zero points of the metric function $g(r)$ and hence 3 horizons of spacetime [100] and five possible configurations shown in Figure 1a [89]. Dependently on the mapping (choice of the observers reference frame) spacetime geometry presents the black (white) hole with three horizons, the internal horizon r_-, the event black (white) hole horizon r_+ and the cosmological horizon r_{++}, two extreme double-horizon states $r_- = r_+$, $r_+ = r_{++}$, and two one-horizon states shown in Figure 1a [100]. Static observers exist in the R-regions $0 \leq r < r_-$ and $r_+ < r < r_{++}$.

The T-regions $r > r_{++}$ open to infinity represent in the relevant mapping $r \to T, t \to u$ the regular homogeneous cosmological T-models of the Kantowski-Sachs type with the vacuum dark fluid [101]. Typical features of these models are the existence of a Killing horizon, beginning of the cosmological evolution with a null bang from the Killing horizon, and the existence of a regular static pre-bang region visible to the cosmological observers [101]. The Kantowski-Sachs observers are shown in Figures 1b and 2.

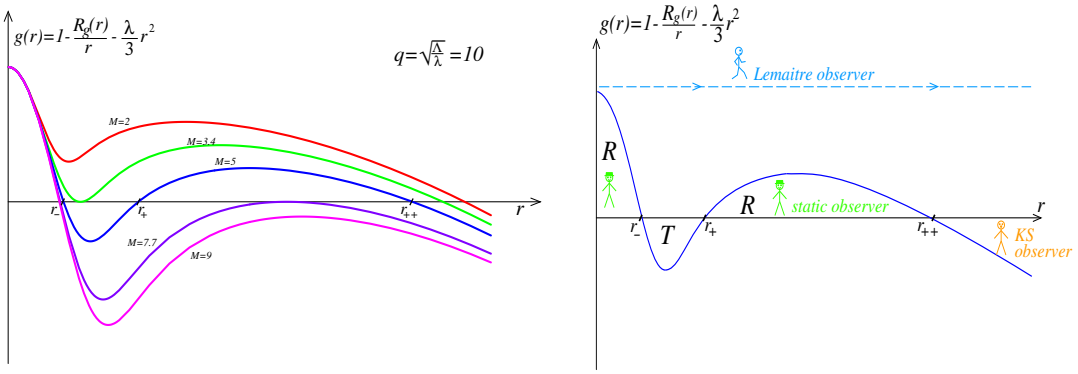

(**a**) (**b**)

Figure 1. (**a**) Five configurations described by (2). (**b**) Observers in the 3-horizons spacetime.

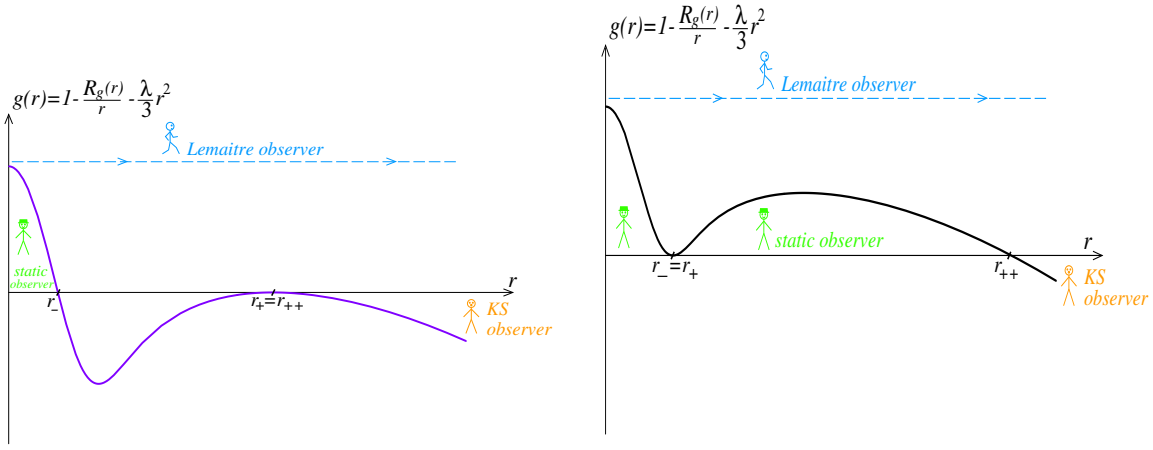

(**a**) (**b**)

Figure 2. Observers in the double horizon spacetimes: (**a**) $r_+ = r_{++}$, (**b**) $r_- = r_+$.

The Lemaître observers on the time-like radial geodesics, shown in Figures 1b and 2, have to their disposal the whole manifold, $0 \leq r \leq \infty$. Transition to their (geodesic) coordinates (R, τ), where R is the congruence parameter of the geodesic family and τ is the proper time along a geodesic, is given by the matrix relating the mapping $[r, t]$ to the mapping $[R, \tau]$ which reads [100]

$$\frac{\partial t}{\partial \tau} = \frac{E(R)}{g(r)}; \ \frac{\partial r}{\partial R} = \sqrt{E^2(R) - g(r)}; \ \frac{\partial r}{\partial \tau} = \pm \frac{\partial r}{\partial R}; \ \frac{\partial t}{\partial R} = \pm \frac{E^2(R) - g(r)}{E(R) g(r)}. \tag{5}$$

The resulting metric has the form [58,100]

$$ds^2 = d\tau^2 - \frac{[E^2(R) - g(r(R,\tau))]}{E^2(R)} dR^2 - r^2(R,\tau) d\Omega^2. \tag{6}$$

3. The Lemaître Class Models for Relaxing Cosmological Constant

3.1. Basic Equations

The cosmological models dominated by the anisotropic vacuum dark energy belong to the Lemaître class models with the anisotropic fluid and are described by the metric [102]

$$ds^2 = d\tau^2 - e^{2\nu(R,\tau)}dR^2 - r^2(R,\tau)d\Omega^2. \tag{7}$$

The coordinates R, τ are the Lagrange (comoving) coordinates. The function $r(R,\tau)$ is called the luminosity distance. For the metric (7) the Einstein equations read [103]

$$8\pi G p_r = \frac{1}{r^2}\left(e^{-2\nu}r'^2 - 2r\ddot{r} - \dot{r}^2 - 1\right), \tag{8}$$

$$8\pi G p_\perp = \frac{e^{-2\nu}}{r}(r'' - r'\nu') - \frac{\dot{r}\dot{\nu}}{r} - \ddot{\nu} - \dot{\nu}^2 - \frac{\ddot{r}}{r}, \tag{9}$$

$$8\pi G\rho = -\frac{e^{-2\nu}}{r^2}\left(2rr'' + r'^2 - 2rr'\nu'\right) + \frac{1}{r^2}\left(2r\dot{r}\dot{\nu} + \dot{r}^2 + 1\right), \tag{10}$$

$$8\pi G T_t^r = \frac{2e^{-2\nu}}{r}\left(\dot{r}' - r'\dot{\nu}\right) = 0. \tag{11}$$

The component T_t^r zeros out in the comoving reference frame, and the Equation (11) yields [104]

$$e^{2\nu} = \frac{r'^2}{1 + f(R)}, \tag{12}$$

where $f(R)$ is an arbitrary integration function. The dots and primes stand for $\partial/\partial\tau$ and $\partial/\partial R$, respectively. Comparison of the metric (6) with the metric (7) shows that (6) corresponds to (7) with $f(R) = E^2(R) - 1$, and $E^2(R) - g(r) = [r'(R,\tau)]^2 = [\dot{r}(R,\tau)]^2$ [100]. It follows that for the case of the vacuum dark fluid with the anisotropic pressures satisfying (1), generic behavior of the Lemaître class cosmological models is determined by the basic properties of the metric function $g(r)$ in (3).

Putting (12) into (8), we obtain the equation of motion [105]

$$\dot{r}^2 + 2r\ddot{r} + 8\pi G p_r r^2 = f(R). \tag{13}$$

Taking into account that $p_r = -\rho$ for a source term (1), the first integration in (13) gives [100]

$$\dot{r}^2 = \frac{2G\mathcal{M}(r)}{r} + f(R) + \frac{F(R)}{r}. \tag{14}$$

A second arbitrary function $F(R)$ should be chosen equal to zero for the models regular at $r = 0$ since $\mathcal{M}(r) \to 0$ as r^3 for $r \to 0$ where $\rho(r) \to \rho_\Lambda < \infty$. The second integration in (13) gives

$$\tau - \tau_0(R) = \int \frac{dr}{\sqrt{2G\mathcal{M}(r)/r + f(R)}}. \tag{15}$$

The new arbitrary function $\tau_0(R)$ is called the bang-time function [106].

For the expanding models $\dot{r} = \sqrt{E^2(R) - g(r)} = r'$ and hence r is a function of $(R + \tau)$. We can therefore choose $\tau_0(R) = -R$. For the small values of r the Equation (15) reduces to

$$\tau + R = \int \frac{dr}{\sqrt{r^2/r_\Lambda^2 + f(R)}} \tag{16}$$

that corresponds to the de Sitter geometry with $r(R,\tau) = r_\Lambda \cosh\left((\tau + R)/r_\Lambda\right)$ for $f(R) < 0$; $r(R,\tau) = r_\Lambda \exp\left((\tau + R)/r_\Lambda\right)$ for $f(R) = 0$; $r(R,\tau) = r_\Lambda \sinh\left((\tau + R)/r_\Lambda\right)$ for $f(R) > 0$.

3.2. Basic Features of the Lemaître Cosmological Models With the Vacuum Dark Energy

For the case $f(R) = 0$ preferred by the observational data ($\Omega = 1$), the cosmological evolution starts from the regular time-like surface $r(R, \tau) = 0$ where the Equation (16) gives [105]

$$r = r_\Lambda e^{(\tau+R)/r_\Lambda}; \;\; e^{2\nu} = r^2/r_\Lambda^2, \tag{17}$$

and the metric (7) takes the FLRW form with the de Sitter scale factor

$$ds^2 = d\tau^2 - r_\Lambda^2 e^{2\tau/r_\Lambda} \left(du^2 + u^2 d\Omega^2 \right), \tag{18}$$

where $u = e^{R/r_\Lambda}$. In accordance with (17), it describes a non-singular non-simultaneous de Sitter bang from the surface $r(\tau + R \to -\infty) = 0$ [100,105], as it is shown in Figure 3 which presents the global structure of spacetime for the most general case of 3 horizons. The regions $\mathcal{RC}$ are the regular regions asymptotically de Sitter as $r \to 0$ at the scale of Λ replacing a singularity; the T-regions $\mathcal{WH}$ and $\mathcal{BH}$ represent the white and black holes; the regions $\mathcal{U}$ are the R-regions restricted by the cosmological horizons r_{++}; the regions $\mathcal{CC}$ are the T-regions asymptotically de Sitter with the background λ as $r \to \infty$. The surfaces $\mathcal{J}_-$ and $\mathcal{J}_+$ are the null (photon) boundaries in the past and the future, respectively. The cosmological evolution starts from the regular de Sitter surface $r = 0$ in $\mathcal{RC}_1$ and goes through $\mathcal{WH}$ and $\mathcal{U}_1$ towards $r \to \infty$ in $\mathcal{CC}_1$.

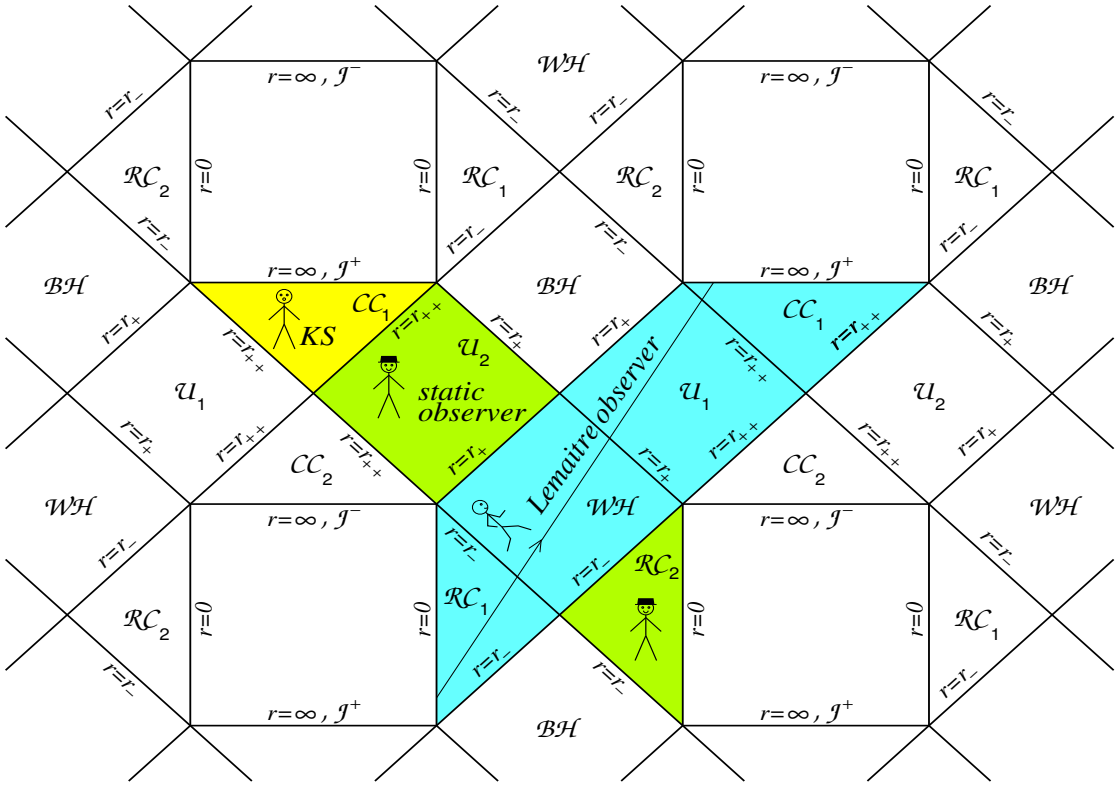

Figure 3. The global structure of the regular spacetime with 3 horizons.

Cosmological evolution is governed by dynamics of pressures. In the spacetime with the de Sitter center the total density monotonically decreases to ρ_λ, hence the total radial pressure $p_r = -\rho$ monotonically increases. Transversal pressure in the case of two vacuum scales evolves from the value $p_\perp = -\rho_\Lambda - \rho_\lambda$ at the inflation to the final value $p_\perp = -\rho_\lambda$, through one maximum in between [100,105]. Typical behavior of pressures (normalized to ρ_Λ) dependently on q is shown

in Figure 4; the variable $\tau + R$ is normalized to the GUT time $t_{GUT} = r_\Lambda/c \simeq 0.8 \times 10^{-35}$ s for $M_{GUT} \simeq 10^{15}$ GeV.

The inflationary stage is followed by a strongly anisotropic Kasner-type stage. As follows from the Lemaître metric in the form (6) corresponding to (7) with $f(R) = E^2(R) - 1$, for any function $f(R)$ the expansion in the transversal direction with $\partial_\tau r > 0$ is accompanied by shrinking in the radial direction where $\partial_R |g_{RR}| < 0$ until $dg(r)/dr < 0$ [100]. For $E^2 = 1$ ($f(R) = 0$) the metric at this stage ($r_\Lambda < r \ll r_\lambda$) takes the form [100,105]

$$ds^2 = d\tau^2 - (\tau + R)^{-2/3} K(R) dR^2 - L(\tau + R)^{4/3} d\Omega^2, \tag{19}$$

where $K(R)$ is a smooth regular function and L is a constant, which depend on the specific form of the density profile and hence on the mass function in (3).

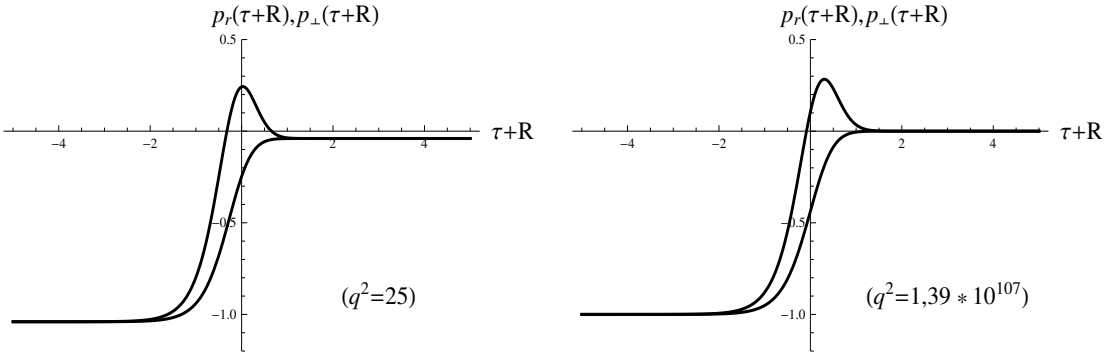

Figure 4. Behavior of p_r (lower curve) and $p_\perp$ (upper curve), at the early and present stages.

The intrinsic anisotropy of the Lemaître class cosmological models is described by the mean anisotropy parameter [107] (for a discussion of the different anisotropy characteristics [108])

$$A = \frac{1}{3H^2} \sum_{i=1}^{3} H_i^2; \quad H_i = \frac{\dot{a}_i(\tau)}{a_i(\tau)}; \quad H = \frac{H_1 + H_2 + H_3}{3}, \tag{20}$$

where $H_i = \dot{a}_i/a_i$ are the directional Hubble parameters corresponding to the scale factors $a_i(\tau)$, and $H = (H_1 + H_2 + H_3)/3$ is the mean Hubble parameter. For the spherically symmetric models with the vacuum dark energy specified by (1), $e^{2\nu} = r'^2$ for $f(R) = 0$, and the scale factors are $a_1 = r'$, $a_2 = a_3 = r$. In terms of the mass function $\mathcal{M}$ the anisotropy parameter takes the form [58,109]

$$A = 2\frac{(\dot{\mathcal{M}}/\mathcal{M}(r) - 3\dot{r}/r)^2}{(\dot{\mathcal{M}}/\mathcal{M} + 3\dot{r}/r)^2}. \tag{21}$$

In the FLRW cosmology the deceleration parameter is introduced on the basis of the Friedmann equations for one scale factor $R(\tau)$. In the case $\Omega = 1$ it reads $q_0 = (\rho + 3p)/2\rho = (1 + 3w)/2$, where w refers to the equation-of-state parameter for an isotropic medium. For $\rho + 3p < 0$ gravitational acceleration becomes repulsive which is responsible for the accelerated expansion. This fact follows directly from the strong energy condition which in general case of an anisotropic medium requires $\rho + \sum p_k \geq 0$. This guarantees, by the Raychaudhuri equation, the attractiveness of gravity [110], and in the cosmological context is responsible for deceleration. Violation of the strong energy condition, $\rho + \sum p_k < 0$, makes gravity repulsive and marks the transition from deceleration to acceleration. In the anisotropic Lemaître cosmology with the vacuum dark energy specified by $T_t^t = T_r^r$ ($p_r = -\rho$), the strong energy condition reads

$$\rho + 2p_\perp \geq 0 \ \rightarrow \ \rho(1 + 2w_\perp) \geq 0. \tag{22}$$

The transition from deceleration to acceleration occurs when $(1 + 2w_\perp) < 0$. In the Lemaître cosmology describing the unverse evolution from the inflationary beginning to the inflationary end with the possible intermediate inflationary stage(s), the maximal number of acceleration-deceleration-acceleration transitions is determined by the numbers of zeros of the pressure $p_\perp$ which is determined by the number of vacuum (de Sitter) scales. In the case of two vacuum scales $p_\perp$ evolves between two inflationary (negative) pressures and can change its sign twice. It results in not more than two transitions: acceleration-deceleration and deceleration-acceleration. Each additional intermediate inflationary stage can add two zeros of $p_\perp$ [58], and hence not more than two additional transitions, acceleration-deceleration and deceleration-acceleration. In the next subsection we consider acceleration-deceleration-acceleration transitions in the model distinguished by the holographic principle.

3.3. The Lemaître Class Models Singled Out by the Holographic Principle

A family of one-horizon spacetimes with the global structure of the de Sitter spacetime contains the special class distinguished by the holographic principle [111] (which leads to the conjecture that a dynamical system can be entirely determined by the data stored on its boundary [112]) as governed by the quantum evaporation of the cosmological horizon that determines the basic characteristics of the final state in the horizon evaporation for any density profile [113].

Typical behavior of the metric function for this class is shown in Figure 5a. Quantum evaporation of the horizon goes towards decreasing the mass M [72]. In this case it ends up in the triple-horizon state $M = M_{cr}$ which is absolutely thermodynamically stable: Its basic generic features are [113] zero temperature, the infinite positive specific heat capacity, the finite entropy, zero transversal pressure, zero curvature, and the infinite scrambling time (the time needed to thermalize information [114]).

Evolution governed by evaporation goes with increasing entropy from the state $M > M_{cr}$ towards the triple-horizon state $M = M_{cr}$ that satisfies three algebraic equations: $g(r_t) = 0$; $g'(r_t) = 0$; $g''(r_t) = 0$, which determine uniquely the basic parameters: the mass M_t, the triple horizon radius r_t, and $q_t = \sqrt{\rho_\Lambda/\rho_\lambda}$, so that the final non-zero value of the vacuum dark energy density ρ_λ is tightly fixed by the quantum evaporation of the cosmological horizon for a chosen vacuum scale for ρ_Λ [113].

With using the density profile [63]

$$\rho(r) = \rho_\Lambda e^{-r^3/r_\Lambda^2 r_g}, \tag{23}$$

which describes the vacuum polarization in the spherically symmetric gravitational field in a simple semiclassical model [78,90], we obtain [113]

$$M_{cr} = 2.33 \times 10^{56}\,\mathrm{g};\ q_{cr}^2 = 1.37 \times 10^{107};\ r_t = 5.4 \times 10^{28}\,\mathrm{cm}. \tag{24}$$

The cosmological evolution is described by the Lemaître metric (7) which can be written as

$$ds^2 = d\tau^2 - b^2(\tau, R)dR^2 - r^2(\tau, R)d\Omega^2, \tag{25}$$

where the second scale factor $b(\tau, R) \equiv e^{\nu(R,\tau)}$ in accordance with (12). Behavior of two scale factors is shown in Figure 5b for the case $f(R) = 0$ $(\Omega = 1)$ [109]. Distances and times are normalized to $r_* = (r_\Lambda^2 r_g)^{1/3} = 1.26 \times 10^{-7}$ cm, and $t_{GUT} \simeq 0.8 \times 10^{-35}$ s with $M_{GUT} \simeq 10^{15}$ GeV.

Due to the isotropy of pressures (see Figure 4), at the very early and late times the behavior of two scale factors is similar (curves run parallel and differ only by constant), the second stage of the parallel running starts at $r_d \simeq 3 \times 10^{27}$ cm and $(\tau + R)_d \simeq 9,5 \times 10^{16}$ s (according to the observational data the vacuum density starts to dominate at the age of about 3×10^9 years). The vacuum density approaches its observed value at the triple horizon r_t at $(\tau + R)_t \simeq 2,9 \times 10^{17}$ s. The metric (7) approaches the FLRW form with the de Sitter scale factor $ds^2 = d\tau^2 - r_t^2 e^{2c\tau/r_t}\left(du^2 + u^2 d\Omega^2\right)$ where $u = e^{R/r_t}$.

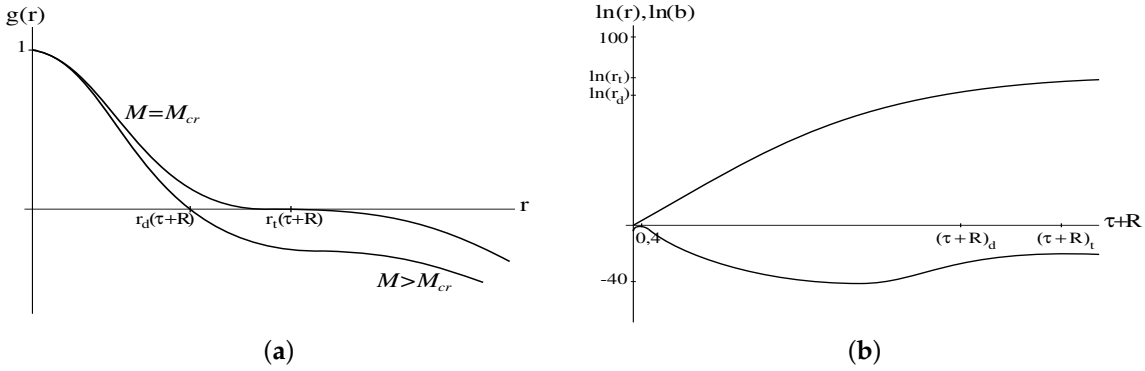

Figure 5. (**a**) Evolution of the metric function during evaporation. (**b**) Behavior of the scale factors: $r(\tau + R)$ (upper curve) and $b(\tau + R)$ (lower curve).

To evaluate the vacuum dark energy density from $q^2_{cr} = \rho_\Lambda/\rho_\lambda$, we adopt $\rho_\Lambda = \rho_{GUT}$. The Grand Unification scale is estimated as $M_{GUT} \sim 10^{15} - 10^{16}$ GeV, which results in the value for the vacuum density ρ_Λ within the range $1.7 \times 10^{-30} gcm^{-3} - 1.7 \times 10^{-26} gcm^{-3}$, respectively.

The observational value $\rho_{\lambda\ (obs)} \simeq 6.45 \times 10^{-30} g\ cm^{-3}$ [11] corresponds, in the considered context, to $M_{GUT} \simeq 1.4 \times 10^{15}$ GeV which gives $\rho_{GUT} = 8.8 \times 10^{77} gcm^{-3}$, $r_\Lambda = 1.8 \times 10^{-25}$ cm. For this scale q^2_{cr} gives the value of the present vacuum density ρ_λ in agreement with its observational value [109].

The behavior of two scale factors and of their derivatives at the early stage of evolution is shown in Figures 6 and 7 [115]. The maximum in the scale factor $b(\tau + r)$ at $\tau + R \simeq 0.4\ t_{GUT} = 0.32 \times 10^{-35}$ s corresponds to the maximum of the transversal pressure at $r \simeq 1.5 \times 10^{-7}$ cm in Figure 4.

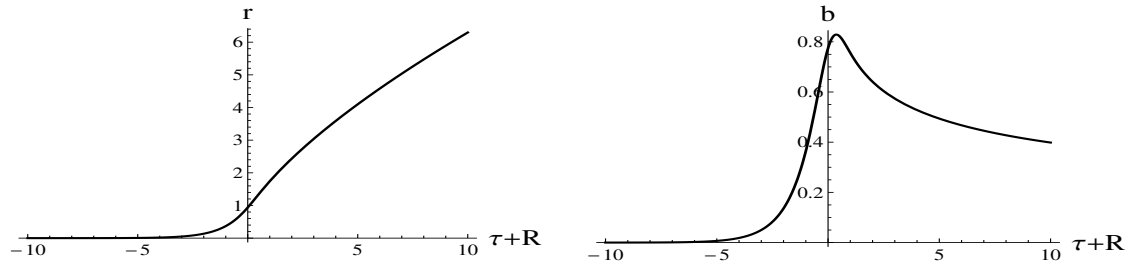

Figure 6. Behavior of the scale factors at the early stage of evolution.

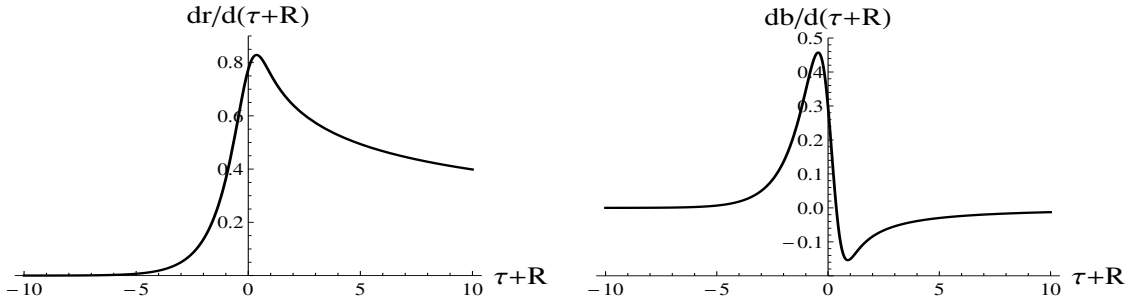

Figure 7. Behavior of the velocities $\dot{r}(\tau + R)$, $\dot{b}(\tau + R)$ at the early stage of evolution.

Behavior of the anisotropy parameter during the whole evolution, shown in Figure 8 [109], was studied numerically with the density profile (23) and the model parameters (24).

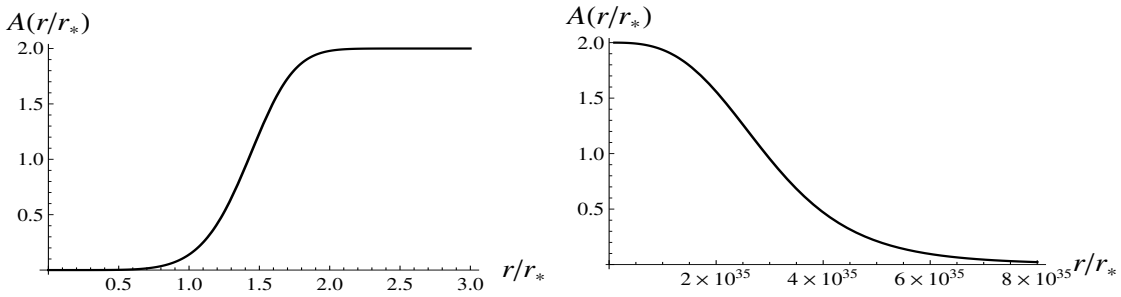

Figure 8. Behavior of the anisotropy parameter at the early and late stages.

The anisotropy develops quickly during the postinflationary stage. At the maximum of $p_\perp$ and $b(\tau + r)$, the anisotropy parameter takes the value $A \simeq 0.4$, grows further achieving $A = 2$ at $r \simeq 2.5 \times 10^{-7}$ cm, and starts to decrease at $r \simeq 6 \times 10^{27}$ cm. The standard estimate $A < 10^{-6}$ is expected to be satisfied already at the recombination epoch, $r \sim 10^{25}$ cm ($z \sim 10^3$). The curve in Figure 7 predicts that the anisotropy starts to satisfy this criterion at approaching $r \sim 10^{28}$ cm when the present vacuum density starts to dominate [109].

In the spacetime with two vacuum scales the pressure $p_\perp$ changes its sign twice [58,100], so that in any triple-horizon model the strong energy condition is violated ($1 + 2w_\perp < 0$ in Equation (22)) in the inflationary stage, and the transition from acceleration to deceleration occurs when satisfaction of the strong energy condition is restored; deceleration changes to acceleration at approaching the current stage of accelerated expansion. The rates of these processes depend essentially on the density profile. For the quickly decreasing density profile (23) the acceleration changes to deceleration after the inflation at $r_1 \simeq 0.4 \times 10^{-7}$ cm, at the essentially anisotropic stage.

4. Summary and Discussion

Responsibility of the spacetime symmetry for reducing the cosmological constant to a certain value in the course of the universe evolution, is suggested on general setting by the algebraic classification for stress-energy tensors which allows for a model-independent definition of a vacuum as a medium and implies the existence of vacua whose symmetry is reduced as compared with the maximally symmetric de Sitter vacuum $p = -\rho$ associated with the Einstein cosmological term. In the spherically symmetric case their stress-energy tensors have the canonical form $T_t^t = T_r^r$ ($p_r = -\rho$) and generate the Lemaître class cosmological models with the anisotropic pressures that allows to describe cosmological evolution by intrinsically dynamical, time-dependent and spatially inhomogeneous vacuum dark energy. In the Lemaître class dark energy models the characteristics of the vacuum dark energy are determined by the algebraic structure of its stress-energy tensor and generically related to the spacetime symmetry. The basic features of the Lemaître class dark energy models are the non-singular non-simultaneous de Sitter bang, followed by the anisotropic Kasner-type stage and directed towards the late-time de Sitter stage, representing the effective relaxation of the cosmological constant from the initial inflationary value Λ to the final late-time inflationary value $\lambda < \Lambda$.

Among these models there is a special class of the one-horizon models distinguished by the holographic principle. The cosmological evolution is governed by the quantum evaporation of the cosmological horizon which determines uniquely the non-zero final value of the cosmological constant in the restoration of the spacetime symmetry to the de Sitter group.

In the case of adopting for the dark energy the density profile representing semi-classically the vacuum polarization in the spherical gravitational field and the GUT scale for the initial vacuum density, its final value appears in agreement with the value given by observations.

Let us note that this special class of models is essentially different from the holographic dark energy models with the isotropic fluid and the postulated density profile. The Lemaître cosmological models are intrinsically anisotropic and describe evolution of the dark energy density represented by

the T_0^0 component of the variable cosmological term whose symmetry is reduced as compared with the Einstein cosmological term.

The anisotropy parameter in the special class of the one-horizon Lemaître dark energy models grows quickly during the postinflationary stage, then stays constant and decreases achieving $A < 10^{-6}$ when the present vacuum density starts to dominate. Astronomical observations suggest that our Universe can be deviated from the isotropy. The observed CMB anisotropy, interpreted as a realization of a statistical process originating in the inflationary era [116–118] admit the statistical anisotropy with the confidence level above 99% [116]. The anisotropy has been constrained at the magnitude level of 2–5% by the SNe Ia data [119], and at the level of 4.4% by the Union2 data and the high-redshift gamma-ray bursts [120]. The deviations from the homogeneity also can be confronted with observations. The influence of inhomogeneities on the cosmological distance measurements has been considered in [121].

The Lemaître class cosmological models provide an appropriate tool for the detailed analysis of the anisotropy and inhomogeneity against observations.

Author Contributions: Authors contributed equally to this work.

Funding: This research received no external funding.

Conflicts of Interest: The authors declare no conflict of interest.

References

1. Riess, A.G.; Kirshner, R.P.; Schmidt, B.P.; Jha, S.; Challis, P.; Garnavich, P.M.; Esin, A.A.; Carpenter, C.; Grashius, R. BV RI light curves for 22 type Ia supernovae. *Astron. J.* **1999**, *117*, 707–724. [CrossRef]
2. Perlmutter, S.; Aldering, G.; Goldhaber, G.; Knop, R.A.; Nugent, P.; Castro, P.G.; Deustua, S.; Fabbro, S.; Goobar, A.; Groom, D.E.; et al. Measurements of Ω and Λ from 42 high-redshift supernovae. *Astrophys. J.* **1999**, *517*, 565–586. [CrossRef]
3. Bahcall, N.A.; Ostriker, J.P.; Perlmutter, S.; Steinhardt, P.J. The cosmic triangle: Revealing the state of the universe. *Science* **1999**, *284*, 1481–1488. [CrossRef]
4. Wang, L.; Caldwell, R.R.; Ostriker, J.P.; Steinhardt, P.J. Cosmic Concordance and Quintessence. *Astrophys. J.* **2000**, *530*, 17–35. [CrossRef]
5. Sullivan, M.; Guy, J.; Conley, A.; Regnault, N.; Astier, P.; Balland, C.; Basa, S.; Carlberg, R.G.; Fouchez, D.; Hardin, D.; et al. SNLS3: Constraints on dark energy combining the supernova legacy survey three-year data with other probes. *Astrophys. J.* **2011**, *737*, 102–121. [CrossRef]
6. Corasaniti, P.S.; Copeland, E.J. Constraining the quintessence equation of state with SnIa data and CMB peaks. *Phys. Rev. D* **2002**, *65*, 043004. [CrossRef]
7. Hannestad, S.; Mortsell, E. Probing the dark side: Constraints on the dark energy equation of state from CMB, large scale structure, and type Ia supernovae. *Phys. Rev. D* **2002**, *66*, 063508. [CrossRef]
8. Bassett, B.A.; Kunz, M.; Silk, J.; Ungarelli, C. A late-time transition in the cosmic dark energy? *Mon. Not. R. Astron. Soc.* **2002**, *336*, 1217–1222. [CrossRef]
9. Tonry, J.L.; Schmidt, B.P.; Barris, B.; Candia, P.; Challis, P.; Clocchiatti, A.; Coil, A.L.; Filippenko, A.V.; Garnavich, P.; Hogan, C.; et al. Cosmological results from high-z supernovae. *Astrophys. J.* **2003**, *594*, 1–24. [CrossRef]
10. Ellis, J. Dark matter and dark energy: Summary and future directions. *Philos. Trans. A* **2003**, *361*, 2607–2627. [CrossRef]
11. Corasaniti, P.S.; Kunz, M.; Parkinson, D.; Copeland, E.J.; Bassett, B.A. Foundations of observing dark energy dynamics with the Wilkinson Microwave Anisotropy Probe. *Phys. Rev. D* **2004**, *70*, 083006. [CrossRef]
12. Weinberg, S. The cosmological constant problem. *Rev. Mod. Phys.* **1989**, *61*, 1–23. [CrossRef]
13. Wheeler, J.A.; Ford, K. *Black Holes and Quantum Foam: A Life in Physics*; W.W. Norton and Co.: New York, NY, USA, 1998.
14. Hawking, S. Spacetime foam. *Nucl. Phys. B* **1978**, *144*, 349–362. [CrossRef]
15. Coleman, S. Why There Is Nothing Rather Than Something: A Theory of the Cosmological Constant. *Nucl. Phys. B* **1988**, *310*, 643–668. [CrossRef]

16. Klebanov, I.; Susskind, L.; Banks, T. Wormholes and the cosmological constant. *Nucl. Phys. B* **1989**, *317*, 665–692 . [CrossRef]
17. Feng, C.J.; Li, X.L. Towards a realistic solution of the cosmological constant fine-tuning problem. *Phys. Rev. D* **2014**, *90*, 103009. [CrossRef]
18. Bousso, R.; Harnik, R.; Kribs, G.D.; Perez, G. Predicting the cosmological constant from the causal entropic principle. *Phys. Rev. D* **2007**, *76*, 043513–043530. [CrossRef]
19. Krauss, L.M.; Dent, J.; Starkman, G.D. Late Time Decay of False Vacuum, Measurement, and Quantum Cosmology. *Int. J. Mod. Phys. D* **2009**, *17*, 2501–2505. [CrossRef]
20. Guendelman, E.I. Non singular origin of the Universe and cosmological constant. *Int. J. Mod. Phys. D* **2012**, *20*, 2767–2771. [CrossRef]
21. Cortes, J.L.; Lopez-Sarrion, J. Fine-tuning problem in quantum field theory and Lorentz invariance: A scalar-fermion model with a physical momentum cutoff. *Int. J. Mod. Phys. A* **2017**, *32*, 1750084. [CrossRef]
22. Adler, R.J. Comment on the cosmological constant and a gravitational alpha. *arXiv* **2011**, arXiv:1110.3358.
23. Ade, P.A.R.; Aghanim, N.; Arnaud, M.; Ashdown, M.; Aumont, J.; Baccigalupi, C.; Banday, A.J.; Barreiro, R.B.; Bartlett, J.G.; Bartolo, N.; et al. Planck 2015 results. *Astron. Astrophys.* **2016**, *594*, A13.
24. Li, Y.H.; Zhang, J.F.; Zhang, X. Testing models of vacuum energy interacting with cold dark matter. *Phys. Rev. D* **2016**, *93*, 023002. [CrossRef]
25. Peracanba, J.S.; Perez, J.D.C.; Gomez-Valent, A. Possible signals of vacuum dynamics in the Universe. *Mon. Not. R. Astron. Soc* **2018**, *478*, 4357–4373.
26. Li, H.L.; Feng, L.; Zhang, J.F.; Zhang, X. Models of vacuum energy interacting with cold dark matter: Constraints and comparison. *arXiv* **2018**, arXiv:1812.00319.
27. Sahni, V.; Starobinsky, A.A. The case for a positive cosmological Lambda term. *Int. J. Mod. Phys. D* **2000**, *9*, 373–444. [CrossRef]
28. Bean, R.; Carroll, S.M.; Trodden, M. Insight into dark energy: Interplay between theory and observation. *arXiv* **2005**, arXiv:astro-ph/0510059.
29. Tanabashi, M.; Hagiwara, K.; Hikasa, K.; Nakamura, K.; Sumino, Y.; Takahashi, F.; Tanaka, J.; Agashe, K.; Aielli, G.; Amsler, C.; et al. Dark Energy. *Phys. Rev. D* **2018**, *98*, 030001.
30. Caldwell, R.R.; Kamionkowski, M. The Physics of Cosmic Acceleration. *Ann. Rev. Nucl. Part. Sci.* **2009**, *59*, 397–429. [CrossRef]
31. Copeland E.J. Models of dark energy. In Proceedings of the Invisible Universe International Conference, Paris, France, 29 June–3 July 2009; AIP: New York, NY, USA, 2010; pp. 132–138.
32. Bamba, K.; Capozziello, S.; Nojiri, S.; Odintsov, S.D. Dark energy cosmology: The equivalent description via different theoretical models and cosmography tests. *Astrophys. Space Sci.* **2012**, *342*, 155–228.
33. Rivera, A.B.; Farieta, J.G. Exploring the Dark Universe: Constraint on dynamical dark energy models from CMB, BAO and Growth Rate Measurements. *arXiv* **2016**, arXiv:1605.01984.
34. Aviles, A.; Bravetti, S.; Capozziello, S.; Luongo, O. Precision cosmology with Padé rational approximations: Theoretical predictions versus observational limits. *Phys. Rev. D* **2011**, *90*, 043531. [CrossRef]
35. Capozziello S.; D'Agostino, R.; Luongo, O. Model-independent reconstruction of f(T) teleparallel cosmology. *Gen. Relativ. Gravit.* **2017**, *49*, 141–162. [CrossRef]
36. Cai, Y.F.; Saridakis, E.N.; Setare, M.R.; Xia, J. Quintom Cosmology: Theoretical implications and Observations. *Phys. Rep.* **2010**, *493*, 1–60. [CrossRef]
37. Capozziello, S.; Predipalumbo, E.; Rubano, C.; Scudellaro, P. Noether symmetry approach in phantom quintessence cosmology. *Phys. Rev. D* **2009**, *80*, 104030. [CrossRef]
38. Mishra, S.; Chakraborty, S. Dynamical system analysis of Quintom Dark Energy Model. *Eur. Phys. J. C* **2018**, *78*, 917–923. [CrossRef]
39. Joyce, A.; Lombriser, L.; Schmidt, F. Dark Energy Versus Modified Gravity. *Ann. Rev. Nucl. Part. Sci.* **2016**, *66*, 95–122. [CrossRef]
40. Cognola, G.; Elizalde, E.; Nojiri, S.; Odintsov, S.D.; Sebastiani, L.; Zerbini, S. Class of viable modified f(R) gravities describing inflation and the onset of accelerated expansion. *Phys. Rev. D* **2008**, *77*, 046009. [CrossRef]
41. Horava P.; Minic, D. Probable Values of the Cosmological Constant in a Holographic Theory. *Phys. Rev. Lett.* **2000**, *85*, 1610–1613. [CrossRef] [PubMed]

42. Thomas, S. Holography Stabilizes the Vacuum Energy. *Phys. Rev. Lett.* **2002**, *89*, 81301–81304. [CrossRef] [PubMed]
43. Setare, M.R. Interacting holographic dark energy model in non-flat universe. *Phys. Lett. B* **2006**, *642*, 1–4. [CrossRef]
44. Li, E.K.; Zhang, Y.; Cheng, J.L. Modified holographic Ricci dark energy coupled to interacting relativistic and non-relativistic dark matter in the nonflat universe. *Phys. Rev. D* **2014**, *90*, 083534. [CrossRef]
45. Wang, S.; Wu, J.; Li, M. Holographic Dark Energy. *Phys. Rep.* **2017**, *696*, 1–58. [CrossRef]
46. Cruz, M.; Lepe, S. Holographic approach for dark energy-dark matter interaction in curved FLRW spacetime. *Class. Quantum Gravity* **2018**, *35*, 155013. [CrossRef]
47. Nojiri, S.; Odintsov, S.D. Covariant Generalized Holographic Dark Energy and Accelerating Universe. *Eur. Phys. J. C* **2017**, *77*, 528. [CrossRef]
48. Cruz, M.; Lepe, S. A holographic cut-off inspired in the apparent horizon. *Eur. Phys. J. C* **2018**, *78*, 994. [CrossRef]
49. Cruz M.; Lepe S. Modeling holographic dark energy with particle and future horizons. *arXiv* **2018**, arXiv:1812.06373.
50. Ade, P.A.R.; Aikin, R.W.; Barkats, D.; Benton, S.J.; Bischoff, C.A.; Bock, J.J.; Brevik, J.A.; Buder, I.; Bullock, E.; Dowell, C.D.; et al. Detection of B-Mode Polarization at Degree Angular Scales by BICEP2. *Phys. Rev. Lett.* **2014**, *112*, 241101. [CrossRef] [PubMed]
51. Anderson, L.; Aubourg, E.; Bailey, S.; Beutler, F.; Bhardwaj, V.; Blanton, M.; Bolton, A.S.; Brinkmann, J.; Brownstein, J.R.; Burden, A.; et al. The clustering of galaxies in the SDSS-III Baryon Oscillation Spectroscopic Survey: Baryon acoustic oscillations in the Data Releases 10 and 11 Galaxy samples. *Mon. Not. R. Astron. Soc* **2014**, *441*, 24–62. [CrossRef]
52. Suzuki, N.; Rubin, D.; Lidman, C.; Aldering, G.; Amanullah, R.; Barbary, K.; Barrientos, L.F.; Botyanszki, J.; Brodwin, M.; Connolly, N.; et al. The Hubble Space Telescope Cluster Supernova Survey: Improving the Dark Energy Constraints and Building an Early-Type-Hosted Supernova Sample. *Astrophys. J.* **2012**, *746*, 85–109. [CrossRef]
53. Sahni, V.; Shafiello, A.; Starobinsky, A. A. Model-independent Evidence for Dark Energy Evolution from Baryon Acoustic Oscillations. *Astrophys. J.* **2014**, *793*, L40–L44. [CrossRef]
54. Bauer, F.; Solà, J.; Štefancic, H. Dynamically avoiding fine-tuning the cosmological constant: the "Relaxed Universe". *J. Cosmol. Astropart. Phys.* **2010**, *1012*, 29. [CrossRef]
55. Bauer, F.; Solà, J.; Štefancic, H. Relaxing a large cosmological constant. *Phys. Lett. B* **2009**, *678*, 427–433. [CrossRef]
56. Elizalde E.; Odintsov, S.D.; Sebastiani, L.; Myrzakulov, R. Beyond-one-loop quantum gravity action yielding both inflation and late-time acceleration. *Nucl. Phys. B* **2017**, *921*, 411-–435. [CrossRef]
57. Anderson, P.R. Attractor states and infrared scaling in de Sitter space. *Phys. Rev. D* **2000**, *62*, 124019. [CrossRef]
58. Bronnikov, K.A.; Dymnikova, I.; Galaktionov, E. Multihorizon spherically symmetric spacetimes with several scales of vacuum energy. *Class. Quantum Gravity* **2012**, *29*, 095025. [CrossRef]
59. Petrov, A.Z. *Einstein Spaces*; Pergamon Press: Oxford, UK, 1969.
60. Stephani, H.; Kramer, D.; MacCallum, V.; Hoenselaers, C.; Herlt, E. *Exact Solutions of Einstein's Field Equations*; Cambridge University Press: Cambridge, UK, 2003.
61. Gliner, E.B.; Dymnikova, I.G. Nonsingular Friedmann cosmology. *Sov. Astron. Lett.* **1975**, *1*, 93–95.
62. Olive K.A. Inflation. *Phys. Rep.* **1990**, *190*, 307–403. [CrossRef]
63. Dymnikova, I. Vacuum nonsingular black hole. *Gen. Relativ. Gravit.* **1992**, *24*, 235–242. [CrossRef]
64. Dymnikova, I.; Galaktionov, E. Vacuum dark fluid. *Phys. Lett. B* **2007**, *645*, 358–364. [CrossRef]
65. Dymnikova, I. The algebraic structure of a cosmological term in spherically symmetric solutions. *Phys. Lett. B* **2000**, *472*, 33–38. [CrossRef]
66. Dymnikova, I.; Galaktionov, E. Dark ingredients in one drop. *Cent. Eur. J. Phys.* **2011**, *9*, 644–653. [CrossRef]
67. Dymnikova, I. Unification of dark energy and dark matter based on the Petrov classification and space-time symmetry. *Intern. J. Mod. Phys. A* **2016**, *31*, 1641005. [CrossRef]
68. Dymnikova, I.; Khlopov, M. Regular black hole remnants and graviatoms with de Sitter interior as heavy dark matter candidates probing inhomogeneity of early universe. *Int. J. Mod. Phys. D* **2015**, *24*, 1545002. [CrossRef]

69. Polnarev, A.G.; Khlopov, M.Y. Cosmology, primordial black holes, and supermassive particles. *Sov. Phys. Uspekhi* **1985**, *28*, 213–232. [CrossRef]
70. MacGibbon, J.H. Can Planck-mass relics of evaporating black holes close the Universe? *Nature* **1987**, *329*, 308–309. [CrossRef]
71. Dymnikova, I. Regular black hole remnants. In Proceedings of the Invisible Universe International Conference, Paris, France, 29 June–3 July 2009; AIP: New York, NY, USA, 2010; pp. 361–368.
72. Dymnikova, I.; Korpusik, M. Regular black hole remnants in de Sitter space. *Phys. Lett. B* **2010**, *685*, 12–18. [CrossRef]
73. Dymnikova, I. Generic Features of Thermodynamics of Horizons in Regular Spherical Space-Times of the Kerr-Schild Class. *Universe* **2018**, *4*, 63. [CrossRef]
74. Dymnikova, I.; Fil'chenkov, M. Graviatoms with de Sitter Interior. *Adv. High Energy Phys.* **2013**, *2013*, 746894. [CrossRef]
75. Gibbons, G.W. *Phantom Matter and the Cosmological Constant*; DAMTP-2003-19; Cambridge University: Cambridge, UK, 2003; arXiv:hep-th/0302199.
76. Boyanovsky, D.; de Vega, H.J.; Schwarz, D.J. Phase transitions in the early and present universe. *Ann. Rev. Nucl. Part. Sci.* **2006**, *56*, 441–500. [CrossRef]
77. Poisson, E.; Israel, W. Structure of the black hole nucleus. *Class. Quantum Gravity* **1988**, *5*, L201–L205. [CrossRef]
78. Dymnikova, I. The cosmological term as a source of mass. *Class. Quantum Gravity* **2002**, *19*, 725–740. [CrossRef]
79. Dymnikova, I. Spherically symmetric space-time with regular de Sitter center. *Int. J. Mod. Phys. D* **2003**, *12*, 1015–1034. [CrossRef]
80. Frolov, V.P.; Markov, M.A.; Mukhanov, V.F. Black holes as possible sources of closed and semiclosed worlds. *Phys. Rev. D* **1990**, *41*, 383–394. [CrossRef]
81. Dymnikova, I. Internal structure of nonsingular spherical black holes. *Ann. Isr. Phys. Soc.* **1997**, *13*, 422–440.
82. Perez, A. Spin foam models for quantum gravity. *Class. Quantum Gravity* **2003**, *20*, R43–R104. [CrossRef]
83. Rovelli, C. *Quantum Gravity*; Cambridge University Press: Cambridge, UK, 2004.
84. Bonanno, A.; Reuter, M. Spacetime structure of an evaporating black hole in quantum gravity. *Phys. Rev. D* **2006**, *73*, 83005–83017. [CrossRef]
85. Nicolini, P. Noncommutative black holes, the final appeal to quantum gravity: A review. *Int. J. Mod. Phys. A* **2009**, *24*, 1229–1308. [CrossRef]
86. Arraut, I.; Batic, D.; Nowakowski, M. A noncommutative model for a mini black hole. *Class. Quantum Gravity* **2009**, *26*, 245006. [CrossRef]
87. Arraut, I.; Batic, D.; Nowakowski, M. Maximal extension of the Schwarzschild spacetime inspired by noncommutative geometry. *J. Math. Phys.* **2010**, *51*, 022503. [CrossRef]
88. Kerr, R.P.; Schild, A. Some algebraically degenerate solutions of Einstein's gravitational field equations. *Proc. Symp. Appl. Math* **1965**, *17*, 199–207.
89. Dymnikova, I.; Soltysek, B. Spherically symmetric space-time with two cosmological constants. *Gen. Relativ. Gravit.* **1998**, *30*, 1775–1793. [CrossRef]
90. Dymnikova, I. De Sitter-Schwarzschild black hole: Its particlelike core and thermodynamical properties. *Int. J. Mod. Phys. D* **1996**, *5*, 529–540. [CrossRef]
91. Dymnikova, I.; Sakharov, A.; Ulbricht, J. Appearance of a minimal length in e^+e^- annihilation. *Adv. High Energy Phys.* **2014**, *2014*, 707812. [CrossRef]
92. Bażański, S.L.; Ferrari, V. Analytic Extension of the Schwarzschild-de Sitter Metric. *Il Nuovo Cimento B* **1986**, *91*, 126–142. [CrossRef]
93. Balaguera Antolinez, A.; Böhmer, C.G.; Nowakowski, M. Scales set by the Cosmological Constant. *Class. Quantum Gravity* **2006**, *23*, 485–496. [CrossRef]
94. Arraut, I.; Batic, D.; Nowakowski, M. Velocity and velocity bounds in static spherically symmetric metrics, *Cent. Eur. J Phys.* **2011**, *9*, 926–938.
95. Vainshtein, A.I. To the problem of nonvanishing gravitation mass. *Phys. Lett. B* **1972**, *39*, 393-–394. [CrossRef]
96. Chkareuli, G.; Pirtskhalava, D. Vainshtein mechanism in Λ_3-theories. *Phys. Lett. B* **2012**, *713*, 99–103. [CrossRef]

97. Babichev, E.; Deffayet, C. An introduction to the Vainshtein mechanism. *Class. Quantum Gravity* **2013**, *30*, 184001. [CrossRef]
98. Arraut, I. On the Black Holes in alternative theories of gravity: The case of non-linear massive gravity. *Int. J. Mod. Phys. D* **2015**, *24*, 1550022. [CrossRef]
99. Arraut, I. The Astrophysical Scales Set by the Cosmological Constant, Black-Hole Thermodynamics and Non-Linear Massive Gravity. *Universe* **2017**, *3*, 45. [CrossRef]
100. Bronnikov, K.A.; Dobosz, A.; Dymnikova, I. Nonsingular vacuum cosmologies with a variable cosmological term. *Class. Quantum Gravity* **2003**, *20*, 3797–3814. [CrossRef]
101. Bronnikov, K.A.; Dymnikova, I. Regular homogeneous T-models with vacuum dark fluid. *Class. Quantum Gravity* **2007**, *24*, 5803–5816. [CrossRef]
102. Lemaître, G. Evolution of the Expanding Universe. *Proc. Natl. Acad. Sci. USA* **1934**, *20*, 12–17. [CrossRef]
103. Landau, L.D.; Lifshitz, E.M. *Classical Theory of Fields*, 4th ed.; Butterworth-Heinemann: Oxford, UK, 1975.
104. Tolman, R.C. Effect of Inhomogeneity on Cosmological Models *Proc. Natl. Acad. Sc. USA* **1934**, *20*, 169–176. [CrossRef]
105. Dymnikova, I.; Dobosz, A.; Filchenkov, M.; Gromov, A. Universes inside a Λ black hole. *Phys. Lett. B* **2001**, *506*, 351–360. [CrossRef]
106. Olson, D.W.; Silk J. Primordial inhomogeneities in the expanding universe. II—General features of spherical models at late times. *Astrophys. J.* **1979**, *233*, 395–401. [CrossRef]
107. Harko, T.; Mak, M.K. Bianchi Type I universes with dilaton and magnetic fields. *Int. J. Mod. Phys. D* **2002**, *11*, 1171–1189. [CrossRef]
108. Bronnikov, K.A.; Chudayeva, E.N.; Shikin, G.N. Magneto-dilatonic Bianchi-I cosmology: Isotropization and singularity problems. *Class. Quantum Gravity* **2004**, *21*, 3389–3403. [CrossRef]
109. Dymnikova, I.; Dobosz, A.; Sołtysek, B. Lemaître Class Dark Energy Model for Relaxing Cosmological Constant. *Universe* **2017**, *3*, 39. [CrossRef]
110. Wald, R.M. *General Relativity*; University of Chicago Press: Chicago, IL, USA; London, UK, 1984.
111. 't Hooft, G. Dimensional reduction in quantum gravity. *arXiv* **1999**, arXiv:9310026.
112. Susskind, L. The World as a hologram. *J. Math. Phys.* **1995**, *36*, 6377–6396. [CrossRef]
113. Dymnikova, I., Triple-horizon spherically symmetric spacetime and holographic principle. *Int. J. Mod. Phys. D* **2012**, *21*, 1242007–12420016. [CrossRef]
114. Sekino, Y.; Susskind, L. Fast scramblers. *High Energy Phys.* **2008**, *810*, 65–80. [CrossRef]
115. Dymnikova, I.; Dobosz, A.; Soltysek B. Lemaître dark energy model singled out by the holographic principle. *Gravit. Cosmol.* **2017**, *23*, 28–34. [CrossRef]
116. Wiaux, Y.; Vielva, P.; Martinez-Gonzalez, E.; Vandergheynst, P. Global universe anisotropy probed by the alignment of structures in the cosmic microwave background. *Phys. Rev. Lett.* **2006**, *96*, 151303–151306. [CrossRef] [PubMed]
117. Marochnik L.; Usikov, D. Inflation and CMB anisotropy from quantum metric fluctuations. *Gravit. Cosmol.* **2015**, *21*, 118–122. [CrossRef]
118. Sharma, M. Raychaudhuri equation in an anisotropic universe with anisotropic sources. *Gravit. Cosmol.* **2015**, *21*, 252–256. [CrossRef]
119. Chang, Z.; Li, X.; Lin, H.-N.; Wang, S. Constraining anisotropy of the universe from different groups of type-Ia supernovae. *Eur. Phys. J. C* **2014**, *74*, 2821–2829. [CrossRef]
120. Chang, Z.; Li, X.; Lin, H.-N.; Wang, S. Constraining anisotropy of the universe from Supernovae and Gamma-ray Bursts. *Mod. Phys. Lett. A* **2014**, *29*, 1450067. [CrossRef]
121. Nikolaev, A.V.; Chervon, S.V. The effect of universe inhomogeneities on cosmological distance measurements. *Gravit. Cosmol.* **2016**, *22*, 208–216. [CrossRef]